Chemistry & Biology, Vol. 11, 915–925, July, 2004, ©2004 Elsevier Ltd. All rights reserved. DOI 10.1016/j.chembiol.2004.04.015

Characterization and Investigation of Substrate Specificity of the Sugar Aminotransferase WecE from *E. coli* K12

Bum-Yeol Hwang,[1] Hwa-Jin Lee,[2] Yung-Hun Yang,[1] Hwang-Soo Joo,[1] and Byung-Gee Kim[1,*]
[1]School of Chemical Engineering and Institute for Molecular Biology and Genetics
[2]Interdisciplinary Program for Biochemical Engineering and Biotechnology
Seoul National University
Seoul 151-742
Korea

Summary

***WecE* gene, encoding a sugar aminotransferase (SAT), has been cloned from *E. coli* K12 and expressed in *E. coli* BL21 (DE3). The enzyme was purified and characterized. WecE used TDP-4-keto-6-deoxy-D-glucose (TDP-D-Glc4O) and L-glutamate as a good amino acceptor and donor, respectively, leading to the production of TDP-4-amino-4,6-dideoxy-D-galactose (TDP-Fuc4N), which was identified by NMR studies. WecE also showed a similar activity for TDP-4-keto 6-deoxy-D-mannose (TDP-D-Man4O), but no activity for GDP-4-keto-6-deoxy-D-mannose (GDP-D-Man4O), suggesting that the nucleotide moiety would become a key determinant to the substrate specificity of amine acceptor for the activity of the SAT. Multiple alignments showed that SATs have four highly conserved motifs located around the active site and could be divided into three subgroups (VI_α, VI_β, and VI_γ) that might be closely related with their substrate specificities.**

Introduction

Amino sugars are unusual sugars usually found as parts of macrolide antibiotics such as tylosin, desosamine, and erythromycin [1–3] widely used for respiratory tract, skin, and genitourinary infections, and as components of the O antigen and the lipopolysaccharide (LPS) present in the outer membrane of gram-negative bacteria [4–6]. These amino sugars are usually synthesized in vivo from keto-sugars by aminotransferases. The involved sugar aminotransferases (SATs) are specially classified into DegT/DnrJ/EryC1/StrS aminotransferase families in the Pfam database [7, 8]. These SATs are mainly discovered in antibiotics producing microbes which belong to Actinomycetales and phathogenic microbes such as *E. coli* O157 and *Vibrio cholerae* [9–13]. As the expression of the genes from the Actinomycetales in *E. coli* is very much limited and the keto-sugars used for the substrate of SATs are not commercially available, only a few SATs have been expressed and characterized until now [14–18]. As a result, the identifications of the SATs are currently relying only on homology sequence analysis [1, 3, 19, 20] and knockout mutations of the candidate genes [2, 21]. Therefore, their detailed characterizations are in great demand.

In the SAT study, understanding amino donor and acceptor substrate specificities is usually our primary concern. Amino donor for the transamination reaction of SAT is usually glutamate, but sometimes glutamine or aspartate can be used as well. Amino acceptors of the SATs are mainly NDP-keto-sugars. Understanding nucleotide moiety- and amine group transferring regio-specificities toward NDP-keto-sugars of the SATs would become a key to synthesizing various amino sugar compounds for carbohydrate moiety of new macrolide antibiotics.

Pyranose, in general, has four possibilities (C2, C3, C4, and C6) of amine substitutions for the hydroxyl group on the backbone carbon of the pyranose ring. Prior to the amination, the hydroxyl group should be changed to keto group using dehydratase, and the the keto-sugar becomes the amino acceptor for the transamination reaction. Per from *V. cholerae* [16], LmbS from *Streptomyces linchlnensis* [22], ArnB from *Salmonella typhimurium* [17], and WecE from *E. coli* act on the position of C4 of pyranose. TylB from *Streptomyces fradiae* [18], DesV from *Streptomyces venezuelae* [23], and MegCII from *Micromonospora megalomicea* [20] act on the position of C3 of pyranose. However, the SAT acting on the position of C6 of pyranose has not been identified yet. In addition, aminations at the C2 position of pyranose do not take place by transaminases but by synthases such as GlmS [24]. In terms of nucleotide specificities of SATs, Per from *V. cholerae* acts on GDP-keto-sugar, ArnB from *S. typhimurium* shows the activity to UDP-keto-sugar, whereas WecE from *E. coli*, TylB from *S. radiae*, and DesV from *S. venezuelae* accept TDP-keto-sugars as substrates. However, few studies of the nucleotide and amine group transferring regio-specificities of the SATs have been performed until now [18, 25]. In-depth understanding of the substrate specificities of the SATs provides invaluable tools for in vivo as well as in vitro enzymatic synthesis of novel antibiotics [26] containing various amino sugars, and development of novel inhibitors for antibacterial therapy [27].

In this study WecE from *E. coli* K12 enabling the synthesis of TDP-4-amino-4,6-dideoxy-D-galactose (TDP-Fuc4N) from TDP-4-keto-6-deoxy-D-glucose (TDP-D-Glc4O) was cloned, expressed, and characterized. TDP-Fuc4N is the intermediate of TDP-4-acetamido-4,6-dideoxy-D-galactose (TDP-Fuc4NAc), which is the sugar component of enterobacterial common antigen (ECA) [28, 29]. The enzyme activity of recombinant WecE was quantitatively analyzed by measuring NAD^+ formation using NADH-dependent L-GDH as a coupling enzyme, and the product TDP-Fuc4N was analyzed by one-dimensional and two-dimensional NMR spectra. In addition, the characterization of WecE, such as the amino donor and acceptor specificities, kinetic parameters, conserved motifs, optimal pH, and temperature were examined. To our knowledge, this is the first de-

*Correspondence: byungkim@snu.ac.kr

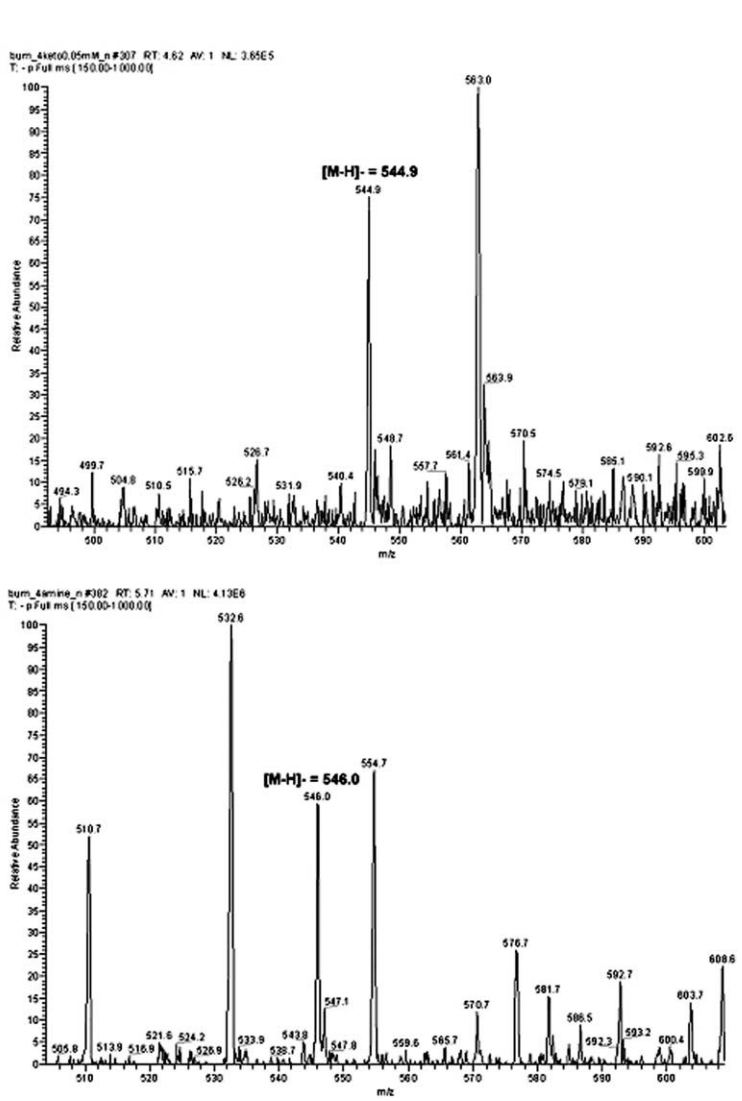

Figure 1. ESI-Mass Spectra of TDP-D-Glc4O and TDP-D-Fuc4N

(A) The ESI-mass peak *m/z* 544.9 corresponds to the mass of the deprotonated TDP-D-Glc4O $[M-H]^-$ and (B) the ESI-mass peak *m/z* 546.0 corresponds to the mass of the deprotonated TDP-D-Fuc4N $[M-H]^-$.

tailed report of nucleotide and pyranose specificities of SAT.

Results

Cloning and Expression of His_6-Tagged WecE

WecE of *E. coli* K12 encoding TDP-4-keto-6-deoxy-D-glucose aminotransferase was cloned into pET24ma containing T7 promoter and C-terminal His_6-tag. The C-terminal His-tagged WecE was overexpressed in soluble form in *E. coli* BL21 (DE3) by IPTG induction for 6 hr at 37°C. The expression was confirmed by SDS-polyacrylamide gel electrophoresis (PAGE) (Supplemental Figure S1A) and the enzyme activity was determined using TDP-D-Glc4O as amino acceptor. The His_6-tagged WecE was purified using immobilized nickel-chelate column chromatography and a hydrophobic interaction column to obtain a homogeneous protein. The molecular mass of the His_6-tagged WecE was about 44 kDa in SDS-PAGE gel, which agreed well with the molecular mass (44,452 Da) deduced from the nucleotide sequence. The molecular mass of the purified His_6-tagged WecE measured by MALDI-TOF linear mode mass spectrometry was 44,465 m/z confirming the SDS-PAGE gel data (Figure S1B). However, according to gel permeation chromatography, its molecular mass was about 180 kDa, suggesting that the enzyme would have a tetrameric structure at native conditions (data not shown). The function of the enzyme was confirmed by the conversion of TDP-D-Glc4O into TDP-Fuc4N using HPLC analysis (data not shown) and ESI-mass spectrometry (Figure 1). The reaction product, i.e., TDP-Fuc4N was identified by 1D ^{1}H- (Figure 2A) and 2D ^{1}H-NMR (Figure 2C) and ESI-mass spectrometry (Figure 1B). Additionally, to confirm its aminotransferase activity, PLP-dependent enzyme inhibitor cocktail comprising 1 mM of hydroxylamine, (aminooxy)acetic acid, and gabaculine was added to the same reaction mixture and its aminotransferase activity was compared with and without the addition of L-glutamate as an amino donor. The activity was completely inhibited in both cases, suggesting that the WecE is a PLP-dependent aminotrans-

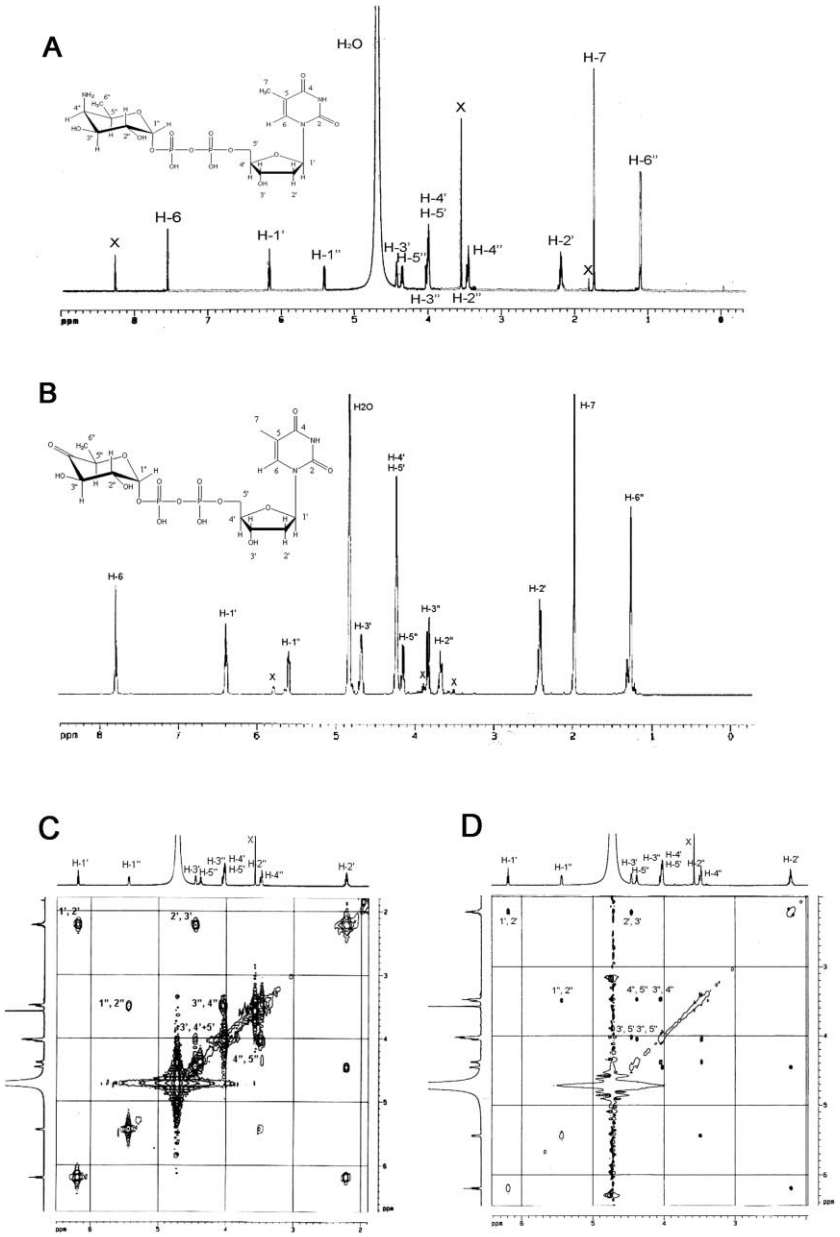

Figure 2. ^{1}H-NMR Spectra of TDP-D-Fuc4N, TDP-D-Glc4O, Two-Dimensional ^{1}H-^{1}H COSY NMR, and NOESY NMR Spectra of TDP-D-Fuc4N at 600 MHz

(A) 10 mg of TDP-D-Fuc4N in D_2O at 25°C and (B) 16 mg of TDP-D-Glc4O in D_2O at 25°C. (C) Shown is a ^{1}H-^{1}H NMR spectra of 10 mg of TDP-D-Fuc4N in the ^{1}H-^{1}H COSY NMR experiment using Bruker Avance-600. (D) Shown is a ^{1}H-^{1}H NMR spectra of 10 mg of TDP-D-Fuc4N in the ^{1}H-^{1}H NOESY NMR experiment using Bruker Avance-600. X indicates an impurity.

ferase (data not shown). We also monitored the absorption spectrum of transaminase. The absorption peaks were found at 330 nm and 417 nm, corresponding to the absorption spectra of E-PMP and E-PLP complexes, respectively (data not shown).

Analysis of TDP-Fuc4N by NMR Spectroscopy

Using 10 units of the purified recombinant WecE protein, about 10 mg of TDP-Fuc4N was synthesized and purified from 22 mg of TDP-D-Glc4O, as described in "Experimental Procedures." The full ^{1}H NMR spectra of TDP-Fuc4N and TDP-D-Glc4O are shown in Figures 2A and 2B, respectively. The spectra reveal the presence of a thymidine and ribose moieties in both compounds with virtually identical chemical shifts and coupling constants. The remaining ^{1}H NMR signals arising from the pyranose differ between the two compounds. The assignment of the pyranose sugar of TDP-Fuc4N in Figure 2 was based upon the COSY analysis (Figure 2C). The cross-peaks from H-1″, H-3″, and H-4″ locate the H-2″ multiplet at 3.50 ppm, the H-4″ multiplet at 3.48 ppm, and the H-5″ multiplet at 4.38 ppm, respectively.

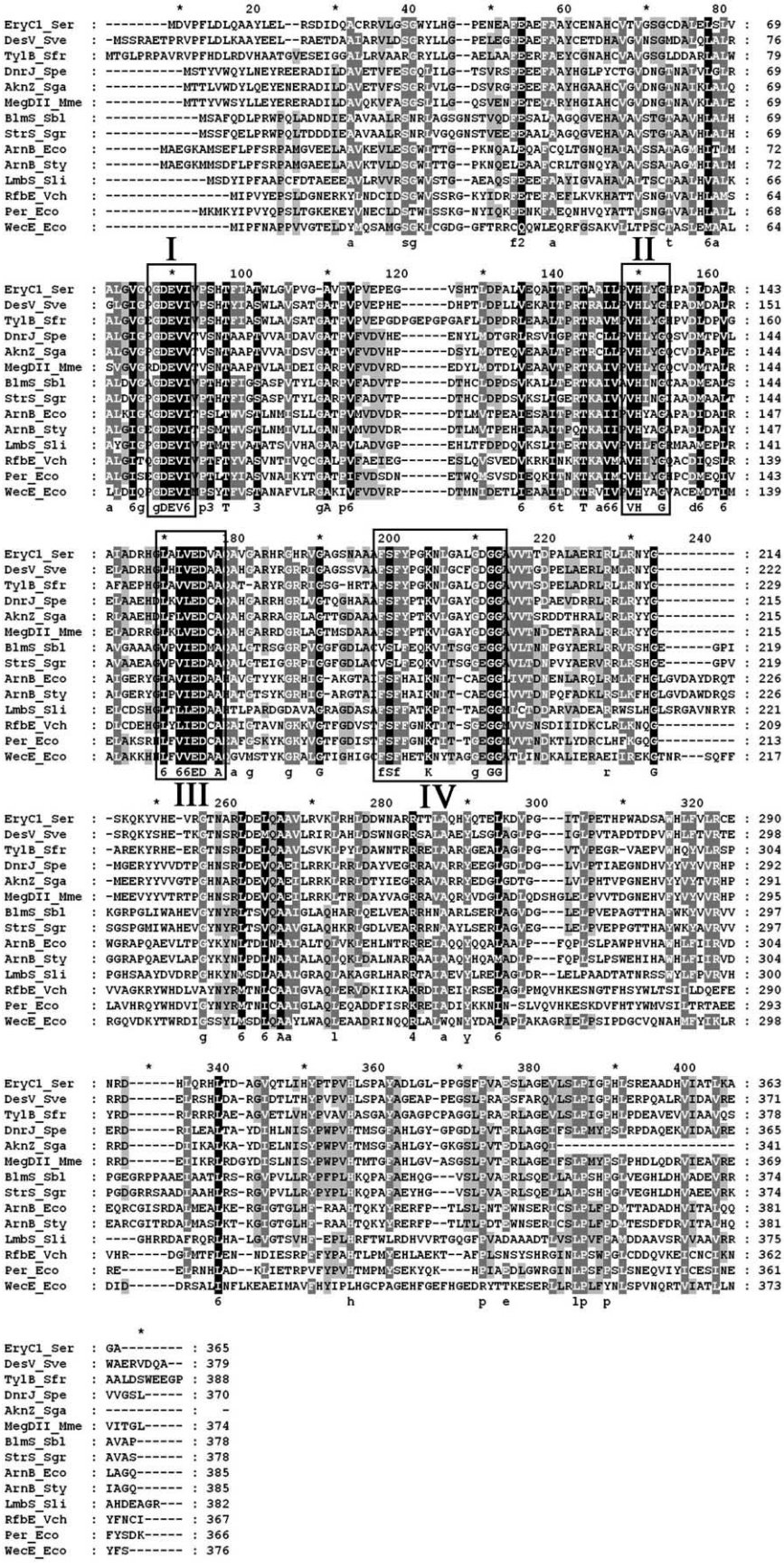

The small $J_{1''2''}$ coupling (3.2 Hz) and the large $J_{2''3''}$ coupling (10.4 Hz) of the pyranose moiety in the NMR spectrum of TDP-Fuc4N demonstrate that this sugar has an equatorially disposed H-1″, and contains axially disposed H-2″ and H-3″ protons [30]. Likewise, the small $J_{3''4''}$ couplings (3.4 Hz) and the small $J_{4''5''}$ coupling (3.5 Hz) of the pyranose moiety in the product indicate that this sugar has an equatorially disposed H-4″ and axially disposed H-3″ and H-5″ protons, suggesting that the amine group at C-4 is disposed axially. The 2D-NOESY data also revealed the expected correlations consistent with this structure (Figure 2D). The cross-peaks from H-1″, H-2″, H-3″, and H-4″ locate the H-2″ multiplet at 3.50 ppm, the H-4″ multiplet at 3.48 ppm, the H-5″ multiplet at 4.38 ppm, and the H-5″ multiplet at 4.38 ppm, respectively.

Sequence Analysis of WecE with Other Sugar Aminotransferases

Using the Clustal W program, the amino acid sequence of WecE from *E. coli* K12 was compared with other homologous SATs. The WecE showed the highest similarity with ArnB from *E. coli* (GenBank accession no. AAM92146, 27% identity and 43% similarity) [17] and ArnB from *Salmonella typhimurium* (GenBank accession no. NP461239, 27% identity and 43% similarity). Other notable SATs with high homology listed with Per from *E. coli* O157:H7 EDL933 (GenBank accession no. AAG57096, 25% identity and 41% similarity) [31], RfbE from *Vibrio cholerae* (GenBank accession no. CAA42137; 23% identity and 43% similarity) [16], EryC1 from *Saccharopolyspora erythraea* (GenBank accession no. S06725; 24% identity and 40% similarity) [3], DesV from *Streptomyces venezuelae* (GenBank accession no. AAC68680; 23% identity and 39% similarity) [21], MegDII from *Micromonospora megalomicea* (GenBank accession no. CAC37809; 24% identity and 40% similarity) [20], and LmbS from *Streptomyces lincolnensis* (GenBank accession no. CAA55764; 26% identity and 41% similarity) [22]. The primary structures of all the proteins compared display a high degree of similarity in length, and have four highly conserved regions, i.e., motif I, motif II, motif III, and motif IV, which are all shown in Figure 3. In addition, there are 19 invariant residues including PLP binding lysine in the multiple alignments of 14 SATs.

The motif I, i.e., (G, D)-D-E-V-(I, V), typically appears in sugar aminotransferases, but not in the other aminotransferases, suggesting the presence of a putative nucleotide binding domain. The motif II, i.e., V-H-X-X-G, would correspond to the active-site region, where the glycine residue (Gly130 for *E. coli* K12 WecE) seems to be positioned at the interface of the PLP binding site and the small binding pocket. The motif III is (I, L,V)-X-(I, L, V)-(I, L, V)-E-D-X-A-(Q, H, E) where the aspartate residue (Asp152 for *E. coli* K12 WecE) is likely to form a salt bridge to N1 of the PLP. And the motif IV is S-(F, L)-(F, Y, H)-X-X-K-$X_{5\text{-}6}$-(E, D)-G-G, where the lysine residue (Lys181 for *E. coli* K12 WecE) is likely to become the active site lysine forming a Schiff base to the PLP [32–34].

Substrate Specificity and Kinetic Constants

The amino donor specificity of WecE was tested with 19 different L-amino acids except L-proline, by fixing TDP-D-Glc4O as the amino acceptor. Among them, L-glutamate showed the highest reactivity, whereas L-glutamine showed relatively lower reactivity. However, the other amino acids showed almost no activity. Likewise, amino acceptor specificity of the enzyme was examined. TDP-D-Glc4O, TDP-D-Man4O, and GDP-D-Man4O were used as the amino acceptors, by fixing L-glutamate as the amino donor. The WecE showed good enzyme activities to TDP-D-Glc4O and TDP-D-Man4O whereas it showed no activity to GDP-D-Man4O. The activity was determined by HPLC analysis and ESI-mass spectrometry (data not shown).

To develop a rapid assay for the SAT kinetic analysis, a UV spectrophotometric method was devised using NADH-dependent L-GDH as a coupling enzyme (Figure 4A) [35]. Initial velocities of the WecE were determined using the standard assay solution of pH 7.5, varying the concentration of TDP-D-Glc4O from 0.01 to 2 mM at 25°C. Maximum enzyme activity was obtained at 1 mM of TDP-D-Glc4O. The Lineweaver-Burk plot obtained from the conversions of TDP-D-Glc4O under the standard assay conditions yielded 0.11 $\pm$ 0.01 (mM) of K_m for TDP-D-Glc4O. The k_{cat} and the catalytic efficiency value (k_{cat}/K_m) were 0.38 $\pm$ 0.01 (s^{-1}) and 3.62 $\pm$ 0.16 ($mM^{-1}s^{-1}$), respectively (data not shown).

Optimum pH and Temperature

Biochemical characterizations of WecE were conducted with the purified enzyme using TDP-D-Glc4O as an amino acceptor and L-glutamate as an amino donor. The effect of pH on the activity of the WecE in crude extracts was examined by using pH values ranging from 5.0 to 9.5. The WecE exhibited more than 80% of its maximum activity at pH 6.0 to 8.0 and very low activity at pH values below 5.0 and above 9.5 (data not shown). The highest activity of His_6-tagged WecE was observed at pH 7.5. The effect of temperature on the activity was studied by using temperature ranging from 20 to 60°C. The WecE activity increased as the temperature increased from 20 to 37°C, but it gradually dropped down to 25% of the maximum activity at 45°C. The highest activity was observed at 37°C (data not shown).

Discussion

The aim of this study was to characterize an SAT, i.e., WecE from *E. coli* K12. Till now, only a few SATs were

Figure 3. Multiple Alignment of the Four Characteristic Consensus Sequences Present in 14 Sugar Aminotransferases

Introduced gaps are shown with hyphens. The four motifs are boxed. Asterisks indicate the position of amino acids. EryC1_Ser (S06725); DesV_Sve (AAC68680); TylB_Sfr (S49052); DnrJ_Spe (B43306); AknZ_Sga (AAF73462); MegDII_Mme (CAC37809); BlmS_Sbl (AAD28515); StrS_Sgr (CAA68523); LmbS_Sli (CAA55764); ArnB_Eco (AAM92146), ArnB_Sty (NP461239), RfbE_Vch (CAA42137); Per_Eco (A99984); WecE_Eco (AAC76796).

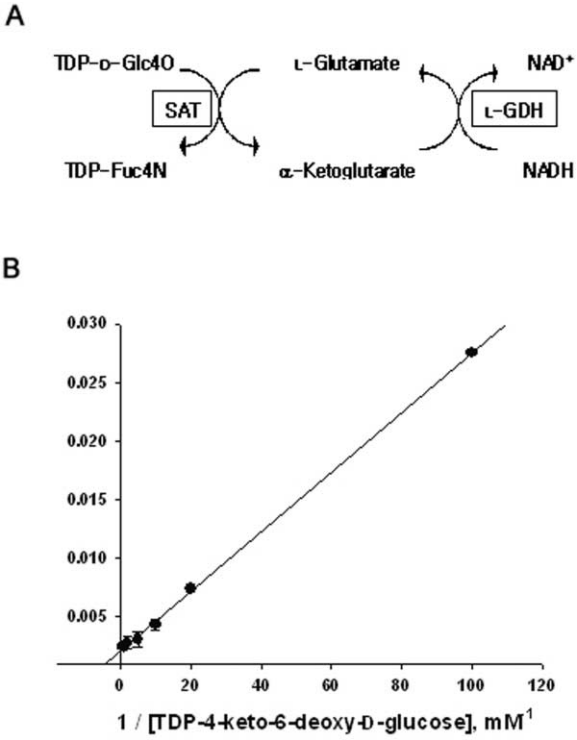

Figure 4. Scheme of the Assay for SATs and Lineweaver-Burk Plot of WecE

(A) Schematic diagram of activity assay for SATs.

(B) WecE activity of the enzyme (1 U) was measured in the presence of the indicated concentrations of TDP-D-Glc4O and 5 mM L-glutamate, 2 μM PLP, 5 mM ammonium chloride, 0.5 mM NADH, L-GDH (0.4 U) at pH 7.5. The concentration of purified WecE was 0.85 mg/ml.

characterized directly by in vitro assays [14, 16–18, 21], and most other SATs were identified by both in vivo mutational study and product assay, confirming that the encoded target proteins are correctly functional in the biosynthesis of the LPS antigens and antibiotics [26, 36, 37]. Therefore, our study will lead to an in-depth understanding of the SATs and their applications.

Aminotransferases could be divided into five subgroups based upon their multiple sequence alignments in the Pfam database. Subgroup "aminotransferase class I and II" includes aspartate aminotransferase, aromatic amino acid aminotransferase, alanine aminotransferase, and histidinol phosphate aminotransferase. Subgroup "aminotransferase class III" includes acetylornithine aminotransferase, ornithine aminotransferase, ω-aminotransferase, and 4-aminobutyrate aminotransferase. Subgroup "aminotransferase class IV" includes D-amino acid aminotransferase and branched-chain amino acid aminotransferase. Subgroup "aminotransferase class V" includes serine aminotransferase and phosphoserine aminotransferase. SATs belong to the subgroup "DegT/DnrJ/EryC1/StrS aminotransferase family." All aminotransferases known to date use the same coenzyme, i.e., PLP, to catalyze transamination reaction, and are differentiated by their substrate specificities originated from their structural differences (Table 1). For example, the aminotransferases in subgroup aminotransferase class I and II accept alanine, dicarboxylic, and aromatic acids as amino donors [38, 39]. The aminotransferases in subgroup aminotransferase class III accept amine and β amino acids [40, 41], and the aminotransferases in subgroup aminotransferase class IV accept D-amino acids and branched-chain amino acids [42, 43] as amino donors. In the case of SATs, amino sugars are particularly used as amino donors [16, 17].

The crystal structure of the enzyme helps understanding of characteristics of the enzyme such as reaction mechanism and substrate specificity [44–46]. In terms of the crystal structure of SAT, until now, only one SAT, ArnB from *S. typhimurium*, was revealed [47]. The ArnB from *S. typhimurium* showed high homology with WecE from *E. coli* K12 (27% identity and 43% similarity), so that the conserved regions of SATs were analyzed based on the 3D structure of ArnB from *S. typhimurium*. Figure 5 shows that the conserved sequences are located around the active site of the enzyme. The His127 of WecE from *E. coli* K12, which corresponds to the conserved His in motif II of SATs, is expected to help stabilize the Asp 152 by hydrogen bonding, so that the side chain of the Asp152 may better form a strong salt bridge with the PLP. The Ala154 of WecE from *E. coli* K12, which corresponds to the conserved Ala in motif II, is expected to help stabilize the Asp152 by hydrogen bonding. The Gln155 of WecE from *E. coli* K12, which corresponds to the conserved Gln/His/Glu in motif II, is expected to form a salt bridge with the 3′-oxygen of the PLP. The Ser176 of WecE from *E. coli* K12, which corresponds to the conserved Ser in the motif IV, is also expected to stabilize the phosphate oxygen of the PLP by hydrogen bonding. The Glu188 of WecE, which corresponds to the conserved Glu/Asp in motif IV, seems to interact with the phosphate group of the PLP. And D-E in motif I seems to be a nucleotide binding motif [48]. The identification of this motif is under further study.

Aminotransferases usually require both amino acceptor and amino donor specificities. In the case of amino acceptors, SATs should recognize keto sugar compounds. WecE from *E. coli* K12 showed high activity for TDP-D-Glc4O as a major amino acceptor, and its activity for GDP-D-Man4O synthesized from GDP-D-Man using the recombinant GDP-D-mannose 4,6-dehydratase from *E. coli* O157:H7 was compared. WecE showed no activity toward GDP-D-Man4O. To investigate which part of the substrate is a more important determinant in substrate recognition of WecE, its activity for TDP-D-Man4O was also compared. TDP-D-Man4O was structurally different from GDP-D-Man only in the nucleotide part. The TDP-D-Man4O was synthesized from TTP and D-mannose-1-phosphate using dTDP-glucose synthase and dTDP-glucose 4,6-dehydratase. WecE displayed good activity toward TDP-D-Man4O (Table S1). We also examined the nucleotide moiety specificity of other SATs such as Per from *E. coli* O157 EDL933 and ArnB from *E. coli* K12. While Per from *E. coli* O157 EDL933 showed activity toward GDP-D-Man4O, it showed no activity toward TDP-D-Glc4O and TDP-D-Man4O (Table S1). In addition, ArnB from *E. coli* K12 showed no activity toward GDP-D-Man4O, TDP-D-Glc4O, and TDP-D-Man4O (data not shown), suggesting

Table 1. Subgroups of Aminotransferases and Their Main Substrates

Subgroup	Enzyme	Main Substrates	
		Amino Donor	Amino Acceptor
I and II	AspAT	L-aspartate	2-ketoglutarate
	AlaAT	L-alanine	2-ketoglutarate
	TyrAT	L-tyrosin	2-ketoglutarate
	HisPAT	L-histidinol-phosphate	2-ketoglutarate
	PheAT	L-phenylalanine	pyruvate
III	AcornAT	*N*-acetyl-L-ornithine	2-ketoglutarate
	OrnAT	L-ornithine	2-ketoglutarate
	ω-AaAT	β-alanine	pyruvate
	GaBaAT	4-aminobutyrate	2-ketoglutarate
	DapaAT	7,8-diaminopelargonate	methylthio-2-oxobutanoate
IV	D-AlaAT	D-alanine	2-ketoglutarate
	BcaaAT	L-leucine	2-ketoglutarate
V	SerAT	L-serine	pyruvate
	PSerAT	3-phospho-L-serine	2-ketoglutarate
DegT/DnrJ/EryC1/StrS (VI)	Per	L-glutamate	4-keto hexose
	TylB	L-glutamate	3-keto hexose
	StsC	L-glutamine	*scyllo*-inosose

AspAT, aspartate aminotransferase; AlaAT, alanine aminotransferase; TyrAT, tyrosin aminotransferase; HisPAT, histidinol-phosphate aminotransferase; PheAT, phenylalanine aminotransferase; AcornAT, acetylornithine aminotransferase; OrnAT, ornithine aminotransferase; ω-AaAT, ω-amino acid aminotransferase; GaBaAT, 4-aminobutyrate aminotransferase; DapaAT, diaminopelargonate aminotransferase; D-AlaAT, D-alanine aminotransferase; BcaaAT, branched-chain amino acid aminotransferase; SerAT, serine aminotransferase; PserAT, phosphoserine aminotransferase.

that the nucleotide moiety is a more important determinant to the activity of WecE.

19 SATs sequences including putative SAT collected through a BLAST search from the NCBI were aligned on the basis of sequence similarity. The phylogenetic tree of SATs showed that SATs could be divided into three subgroups (VI_α, VI_β, and VI_γ) (Figure 5). The subgroup VI_α is composed of WecE from *E. coli*, RfbE from *V. chorelae*, and ArnB from *E. coli*, and so on. These SATs in the subgroup VI_α would act on NDP-4-keto sugars. The SATs in the subgroup VI_β such as DesV from *S. venezuelae*, TylB from *S. fradiae*, and EryC1 from *S. erythraea* would act on NDP-3-keto sugars. And the SATs in the subgroup VI_γ would act on *scyllo*-inosose. Therefore, the sequence similarities between SATs seem to be closely related with their substrate specificities.

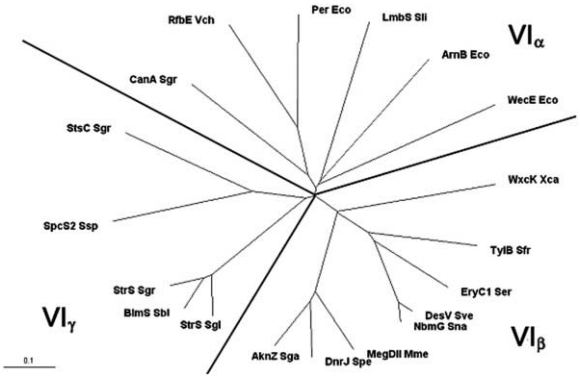

Figure 5. Phylogenetic Tree of Sugar Aminotransferases

The multiple alignments were carried out using the Clustal W program and the figure was generated using the TreeView program. EryC1_Ser (S06725); DesV_Sve (AAC68680); TylB_Sfr (S49052); DnrJ_Spe (B43306); AknZ_Sga (AAF73462); MegDII_Mme (CAC37809); BlmS_Sbl (AAD28515); StrS_Sgr (CAA68523); LmbS_Sli (CAA55764); ArnB_Eco (AAM92146), RfbE_Vch (CAA42137); Per_Eco (A99984); WecE_Eco (AAC76796), CanA_Sgr (CAC22113), WxcK_Xca (AAK53470), NbmG_Sna (AAM88356), SpcS2_Ssp (AAD28492), StsC_Sgr (CAA70012), StrS_Sgl (CAA07383).

In terms of amino donors, WecE from *E. coli* K12 showed the highest activity for L-glutamate, and then, L-glutamine, whose activity was approximately 65% of that for L-glutamate. WecE showed relatively narrow amino donor specificity compared with the aminotransferases which belong to the other families [49, 50]. Likewise, RfbE from *Vibrio cholerae* and ArnB from *E. coli* accept L-glutamate as the main amino donor and their amino donor specificity is only restricted to L-glutamate and L-glutamine [16, 51]. However, StsC from *Streptomyces griseus* and BtrS from *Bacillus circulans* are known to prefer L-glutamine as an amino donor [14, 52].

Significance

Although amino sugar compounds are valuable compounds in pharmaceutical and chemical industry, their chemical synthesis is very difficult due to the need for multistep reactions of protection and deprotection. One efficient way of producing such amino sugar compounds is via SAT reaction. This study unraveled the nucleotide and sugar moiety specificity of SAT for the first time. More profound understanding of nucleotide moiety- and regio-specificity of SAT enables us to control them and hence to provide great freedom to make various amino sugar compounds. The multiple alignments among SATs showed that there were four highly conserved motifs that are located around the active site. SATs could be divided into three subgroups (VI_α, VI_β, and VI_γ) that might be closely related with their substrate specificities.

Table 2. *E. coli* Strains and Plasmids Used in This Study

	Strain or Plasmid	Relevant Properties	Source or Reference
Strains	DH5α	F⁻ φ80*lacZ* M15 *endA recA hsdR*($r_K^-m_K^-$) *supE thi gyrA relA* Δ(*lacZYA-argF*)U169	laboratory stocks
	BL21 (DE3)	F⁻ *ompT hsdS*$_B$ ($r_B^-m_B^-$) *gal dcm*	Novagen
	K12	wild-type	laboratory stocks
	O157:H7 EDL933	*fliC*$_{H7}$ *stx1 stx*$_2$ *eae*$_A$ *hly*$_{933}$	ATCC 700927
Plasmids	pET24ma	p15A replication origin, T7 lac promoter; C-terminal His-tag coding, kan^R	Sourdive D.
	pET15b	pBR322 replication origin, T7 lac promoter, N-terminal His-tag coding, amp^R	Novagen
	pRSET′B′	pUC replication origin, T7 promoter, N-terminal His-tag coding, amp^R	Invitrogen
	pJWEC	pET24ma carrying PCR product of WecE from *E. coli* K12	this work
	pYH303	pET24ma carrying PCR product of GMD from *E. coli* O157:H7	this work
	pJPER	pET24ma carrying PCR product of Per from *E. coli* O157:H7 EDL933	this work
	pHBY31	pET24ma carrying PCR product of ArnB from *E. coli* K12	this work
	pET15b::tmk	pET15b carrying PCR product of dTMP kinase from *E. coli* K12	[53]
	pET24ma::ack	pET 24ma carrying PCR product of acetate kinase from *E. coli* K12	[53]
	pET24ma::tgs	pET24ma carrying PCR product of dTDP-glucose synthase from *E. coli* K12	[53]
	pRSETB::dh	pRSET′B′ carrying PCR product of dTDP-glucose 4,6-dehydratase from *Salmonella typhimurium*	[53]

Experimental Procedures

Bacterial Strains, Plasmids, and Growth Conditions

Bacterial strains and plasmids used in this study are listed in Table 2. *E. coli* cells were grown at 37°C in Luria-Bertani (LB) medium with shaking or on LB agar plates supplemented with 1.5% agar. When appropriate, kanamycin was added at 50 μg/ml.

The expression plasmids pJWEC coding for His_6-tagged sugar aminotransferase WecE were constructed as follows: The forward and backward primers for WecE were 5′-CGCGGATCCGAATTCATTCCATTTAACGCACCGCCG-3′ and 5′-GTGGTGGTGCTCGAGGGAAAAGTAGTTCAACAAAGT-3′ (restriction sites are underlined), respectively. These primers were used to amplify 1,131-bp DNA fragment from a genomic DNA of *E. coli* K12. PCR was carried out in a GeneAmp PCR 2400 (Perkin-Elmer) with 30 cycles of denaturation for 30 s at 94°C, annealing for 30 s at 55°C, and extension for 60 s at 72°C, followed by a 5 min extension period at 72°C. The amplified PCR products were digested by EcoRI-XhoI and the resulting fragments were inserted into the corresponding sites of pET24ma. The pJWEC was sequenced to confirm that the sequences of the inserts were identical to that of the *wecE* gene. pYH303, pJPER, and pHBY301 were constructed by similar procedures. The primers for ArnB (5′-GATATACATATGGCGGAAGGAAAGCAA and 5′-GTGGTGCTCGAGT TGTCCTGCGAGTTGCTG), GMD (5′-GAGGAATAACATATGTCAAAAGTCGCTCTCATC-3′ and 5′-GTTTACAAGCTTTTATGACTCCAGCGCGATC-3′), and Per (5′-CGCGGATCCGAATTCAAAATGAAATATATACCAGTT-3′ and 5′-GTGGTGGTGC TCGAGTTTATCA CTATAAAATTCGTT-3′), which were modified to contain NdeI-XhoI (pHBY31), NdeI-HindIII (pYH301), and EcoRI-XhoI (pJPER) recognition sites to facilitate cloning in frame into expression vector pET24ma, were synthesized.

Chemicals and Enzymes

L-Glutamic dehydrogenase (L-GDH), TTP, and other chemicals were obtained from Sigma (St. Louis, MO). TDP-D-Glc4O was synthesized from TMP and D-glucose-1-phosphate by dTMP kinase, acetate kinase, dTDP-glucose synthase, and dTDP-glucose 4,6-dehydratase [53]. TDP-4-keto-6-deoxy-D-mannose (TDP-D-Man4O) was synthesized from TTP and D-mannose-1-phosphate by dTDP-glucose synthase and dTDP-glucose 4,6-dehydratase. And GDP-4-keto-6-deoxy-D-mannose (GDP-D-Man4O) was synthesized from GDP-D-mannose (GDP-D-Man) by GDP-D-mannose 4,6-dehydratase. Restriction enzymes, DNA-modifying enzymes, and other molecular reagents were obtained from New England Biolabs (Beverly, MA), Roche Biochemical (Indianapolis, IN), Qiagen (Hilden, Germany), and Genenmed (Pittsburgh, PA).

Overexpression and Purification of His_6-Tagged WecE in *E. coli*

For overexpression of His_6-tagged WecE, *E. coli* BL21 (DE3) was transformed with pJWEC. The resulting transformants were grown in LB medium (containing 50 μg/ml of kanamycin) at 37°C until the optical density at 600 nm reached 0.6. Then they were induced with 0.4 mM isopropyl-β-D-thiogalactopyranoside (IPTG) at 37°C for 6 hr. Cells were harvested by centrifugation at 7,000 × g for 15 min at 4°C. The cell pellets were washed with phosphate buffered saline (PBS) buffer (pH 7.2). The cells were resuspended in 50 mM phosphate buffer (pH 7.2) containing 2 mM of EDTA, 1 mM of phenylmethanesulfonyl fluoride (PMSF), 20 μM pyridoxal phosphate (PLP), and 0.01% (v/v) of 2-mercaptoethanol. The cells were then disrupted by sonication, and the cell debris was removed by centrifugation at 15,000 × g for 30 min at 4°C to obtain a crude cell extract.

The His_6-tagged fusion protein was purified from *E. coli* BL21 (DE3) with Ni-NTA agarose resin from Qiagen (Hilden, Germany). Centrifugations and column chromatographies were carried out at 4°C. For His_6-tagged WecE purification, the crude cell extract was passed directly over a column containing 10 ml of Ni-NTA agarose resin. After the column was washed with 50 ml of 50 mM sodium phosphate buffer (pH 8.0) containing 20 mM imidazole, the C-terminal His_6-tagged WecE was eluted with 20 ml of 50 mM sodium phosphate buffer (pH 8.0) containing 200 mM imidazole buffer. The elution solution containing partially purified His_6-tagged WecE was concentrated by an ultrafiltration unit using Centriplus YM-30 (Millipore, Bedford, MA) with molecular mass cutoff of 30 kDa. The resulting preparation was further purified with FPLC (Amersham Biociences, Piscataway, NJ) at a flow rate of 1 ml/min on a Phenyl Sepharose 6 Fast Flow column (Amersham Biosciences). The enzyme was eluted with a negative linear gradient of 0.6 to 0 M ammonium sulfate in 20 mM potassium phosphate (pH 7.0). The purified

WecE was identified by sodium dodecyl sulfate (SDS)-polyacrylamide gel electrophoresis (PAGE) done by Laemmli's method [54].

Molecular Mass Determination by Size-Exclusion Chromatography

The molecular mass of the native enzyme was determined by size-exclusion chromatography with a Sephacryl S-200 (Amersham Biosciences). The column was equilibrated and eluted with 150 mM sodium chloride in 50 mM sodium phosphate buffer (pH 7.0) and calibrated with apoferritin (M_r = 443,000), alcohol dehydrogenase (M_r = 150,000), bovine serum albumin (M_r = 66,000), carbonic anhydrase (M_r = 29,000), and cytochrome *c* (M_r = 12,400).

Enzyme Assays

The activity of WecE was assayed with His_6-tag purified enzyme. The activity of WecE was determined at 25°C using NADH-dependent L-GDH as a coupling enzyme. Under optimized standard conditions, the assay mixture comprised 50 mM potassium phosphate buffer (pH 7.5), 2 mM TDP-D-Glc4O, 5 mM L-glutamate, 2 μM PLP, 5 mM ammonium chloride, 0.5 mM NADH, L-GDH (0.4 U), and 20 μl purified WecE solution in a total volume of 200 μl. The reaction was started by adding WecE to the reaction mixture. The reduction in the absorbance of NADH at 340 nm was monitored continuously with a Multiskan Spectrum Microplate Spectrophotometer (Thermo Labsystems, Vantaa, Finland). One unit of enzyme activity represents 1 μmol of NADH consumed per min. Protein concentrations were determined by the method described in the Bradford assay [55] with bovine serum albumin as the standard.

For the investigation of amino donor specificity of WecE, 50 μl of assay mixture containing 50 mM phosphate buffer (pH 7.5), 2 mM TDP-4-keto-6-deoxy-D-glucose as amino acceptor, 4 mM L-amino acids as amino donors, 2 μM PLP, and the enzyme was used. The reaction was started by the addition of the enzyme, and the reduction of the substrate TDP-4-keto-6-deoxy-D-glucose was measured using the HPLC system (Waters 660, USA) equipped with a UV detector (at 254 nm) and CarboPac PA1 column (4 × 250 mm) (Dionex, Sunnyvale, CA) after stopping the reaction by boiling for 3 min. Elution was carried out with 0.2 M ammonium phosphate solution at a flow rate of 0.8 ml/min and room temperature.

Determination of pH and Temperature Optima

The enzyme activity was determined within a pH range of 5.0 to 9.5. Reaction buffers containing 100 mM sodium acetate (pH 5.0 to 6.0), 100 mM potassium phosphate (pH 6.0 to 8.0), and 100 mM boric acid (pH 8.0 to 9.5), respectively, were used for the enzyme assay. The optimum temperature of the WecE reaction was determined in 100 mM phosphate buffer (pH 7.5) within a range of 20°C to 60°C.

Enzymatic Synthesis and Purification of TDP-Fuc4N

For a single reaction for 12 hr at 37°C, a 20 ml reaction mixture containing the purified recombinant WecE, 2 mM TDP-D-Glc4O, 4 mM L-Glu, and 10 μM PLP in buffer consisting of 50 mM phosphate buffer (pH 7.5) was used. Proteins were removed by passing through an ultrafiltration unit using Centriplus YM-10 (Millipore, Bedford, MA). The reaction product was purified with FPLC (Amersham Biosciences) at a flow rate of 3 ml/min on a column packed with DOWEX 1 × 2-400 ion exchange resin (Sigma-Aldrich). The process was monitored by measuring the absorbance at 254 nm, and the fractions containing the desired product, TDP-Fuc4N, were pooled and concentrated by lyophilization. It was further purified with HPLC on a CarboPac PA1 column. Elution was performed with 20 mM ammonium phosphate solution. The fractions containing the desired product, i.e., TDP-Fuc4N, were pooled and followed by lyophilization to give the pure compound.

Mass Spectrometry

The TDP-D-Glc4O, TDP-D-Man4O, GDP-D-Man4O, and TDP-Fuc4N were determined by mass spectrometry with ESI-mass spectrometry (ThermoFinnigan, CA). And the molecular mass of His_6-tagged WecE was determined by matrix-assisted laser desorption ionization–time of flight (MALDI-TOF) mass spectrometry (Biflex IV, Bruker, Germany).

NMR Spectroscopy

TDP-Fuc4N (10 mg) was dissolved in 0.6 ml of 99% D_2O in a 5 mm NMR tube. One dimensional ^1H and two-dimensional ^1H-^1H COSY and ^1H-^1H NOESY NMR spectra were obtained using Avance-600 (Bruker) at 298 K. ^1H chemical shift of H_2O was 4.72 ppm. ^1H NMR of TDP-Fuc4N δ 7.58 (s, 1 H, H-6), 6.19 (t, 1 H, J = 7.0 Hz, H-1′), 5.44 (dd, 1 H, J = 10.4 and 3.2 Hz, H-1″), 4.47-4.45 (m, 1 H, H-3′), 4.38 (m, 1H, H-5″), 4.06–4.02 (m, 4 H, H-3″, H-4′, H-5′), 3.51–3.49 (m, 1 H-2″), 3.48 (dd, 1 H, J = 3.5 and 3.4 Hz, H-4″), 2.23–2.21 (m, 2 H, H-2a', H-2b'), 1.77 (s, 3 H, H-7), 1.13 (d, 3 H, J = 6.8 Hz, H-6″).

Database Searching, Sequence Retrieval, and Sequence Comparisons

All database searches were performed by using the basic local alignment search tool (BLAST) programs [56, 57] from the NCBI BLAST website (http://www.ncbi.nlm.nih.gov/BLAST/). Multiple alignments of proteins and protein superfamily assignments were performed by using Clustal W [58, 59] v. 1.8 for the Microsoft Windows and Pfam website (http://www.sanger.ac.uk/Software/Pfam/), respectively. The nucleotide accession numbers for the sequence of *wecE*, *tmk*, *ack*, *rffH*, *rfbB*, and *gmd* are AAC76796, AAB06878, NP_416799, P27831, AAL21001, and AAG57113, respectively.

Supplemental Data

Supplemental Figures and Tables can be found at http://www.chembiol.com/cgi/content/full/11/7/915/DC1.

Acknowledgments

We are grateful to Professor Jae Kyung Sohng, Professor Hei Chan Lee, and Professor Kwangkyoung Liou at Sun Moon University for their helpful suggestions and discussions. We are grateful to GeneChem Inc. (Taejon, Korea) for the supply of TDP-D-Glc4O. This research was partially supported by Nano Bioelctronics & System Research Center supported by KOSEF, the Brain Korea 21 program of Korea, and IMT-2000 (Ministry of Commerce, Industry and Energy, Korea).

Received: February 3, 2004
Revised: March 26, 2004
Accepted: April 7, 2004
Published: July 23, 2004

References

1. Merson-Davies, L.A., and Cundliffe, E. (1994). Analysis of five tylosin biosynthetic genes from the *tyllBA* region of the *Streptomyces fradiae* genome. Mol. Microbiol. *13*, 349–355.
2. Summers, R.G., Donadio, S., Staver, M.J., Wendt-Pienkowski, E., Hutchison, C.R., and Katz, L. (1997). Sequencing and mutagenesis of genes from the erythromycin biosynthetic gene cluster of *Sacchropolyspora erythraea* that are involved in L-mycarose and D-desosamine production. Microbiol. *143*, 3251–3262.
3. Dhillon, N., Hale, R.S., Cortes, J., and Leadlay, P.F. (1989). Molecular characterization of a gene from *Saccharopolyspora erythraea* (*Streptomyces erythraeus*) which is involved in erythromycin biosynthesis. Mol. Microbiol. *3*, 1405–1414.
4. Awram, P., and Smit, J. (2001). Identification of lipopolysaccharide O antigen synthesis genes required for attachment of the S-layer of *Caulobacter crescentus*. Microbiol. *147*, 1451–1460.
5. Bastin, D.A., and Reeves, P.R. (1995). Sequence and analysis of the O antigen gene (rfb) cluster of *Escherichia coli* O111. Gene *164*, 1451–1460.
6. Nesper, J., Kraiß, A., Schild, S., Blaß, J., Klose, K.E., Bockemühl, J., and Reidl, J. (2002). Role of *Vibrio cholerae* O139 surface polysaccharides in intestinal colonization. Infect. Immun. *70*, 2419–2433.
7. Sonnhammer, E.L., Eddy, S.R., and Durbin, R. (1997). Pfam: a comprehensive database of protein domain families based on seed alignments. Proteins *28*, 405–420.
8. Bateman, A., Birney, E., Cerruti, L., Durbin, R., Etwiller, L., Eddy, S.R., Griffiths-Jones, S., Howe, K.L., Marshall, M., and Sonn-

hammer, E.L. (2002). The Pfam protein families database. Nucleic Acids Res. *30*, 276–280.

9. Gil, J.A., and Campelo-Diez, A.B. (2003). Candicidin biosynthesis in *Streptomyces griseus*. Appl. Microbiol. Biotechnol. *60*, 633–642.
10. Shimizu, T., Yamasaki, S., Tsukamoto, T., and Takeda, Y. (1999). Analysis of the genes responsible for the O-antigen synthesis in enterohaemorrhagic *Escherichia coli* O157. Microb. Pathog. *26*, 235–247.
11. Bilge, S.S., Vary, J.C., Jr., Dowell, S.F., and Tarr, P.I. (1996). Role of the *Escherichia col*i O157:H7 O side chain in adherence and analysis of an *rfb* locus. Infect. Immun. *64*, 4795–4801.
12. Godfroid, F., Cloeckaert, A., Taminiau, B., Danese, I., Tibor, A., de Bolle, X., Mertens, P., and Letesson, J.J. (2000). Genetic organisation of the lipopolysaccharide O-antigen biosynthesis region of *brucella melitensis* 16M (*wbk*). Res. Microbiol. *151*, 655–668.
13. Vorhölter, F.J., Niehaus, K., and Pühler, A. (2001). Lipopolysaccharide biosynthesis in *Xanthomonas campestris* pv. *campestris*: a cluster of 15 genes is involved in the biosynthesis of the LPS O-antigen and the LPS core. Mol. Genet. Genomics *266*, 79–95.
14. Ahlert, J., Distler, J., Mansouri, K., and Piepersberg, W. (1997). Identification of *stsC*, the gene encoding the L-glutamine:*scyllo*-inosose aminotransferase from streptomycin-producing Streptomycetes. Arch. Microbiol. *168*, 102–113.
15. Tamegai, H., Eguchi, T., and Kakinuma, K. (2002). First identification of *Streptomyces* genes involved in the biosynthesis of 2-deoxystreptamine-containing aminoglycoside antibiotics-Genetic and evolutionary analysis of L-glutamine:2-deoxy-scyllo-inosose aminotransferase genes. J. Antibiot. (Tokyo) *55*, 1016–1018.
16. Albermann, C., and Piepersberg, W. (2001). Expression and identification of the RfbE protein from *Vibrio cholerae* O1 and its use for the enzymatic synthesis of GDP-D-perosamine. Glycobiology *11*, 655–661.
17. Breazeale, S.D., Ribeiro, A.A., and Raetz, C.R. (2003). Origin of lipid A species modified with 4-amino-4-deoxy-L-arabinose in polymyxin-resistant mutants of *Escherichia coli*. An aminotransferase (ArnB) that generates UDP-4-deoxyl-L-arabinose. J. Biol. Chem. *278*, 24731–24739.
18. Chen, H., Yeung, S.-M., Que, N.L.S., Müller, T., Schmidt, R.R., and Liu, H.-W. (1999). Expression, purification and characterization of TylB, an aminotransferase involved in the biosynthesis of mycaminose. J. Am. Chem. Soc. *121*, 7166–7167.
19. Quiros, L.M., Aguirrezabalaga, I., Olano, C., Mendez, C., and Salas, J.A. (1998). Two glycosyltransferases and a glycosidase are involved in oleandomycin modification during its biosynthesis by *Streptomyces antibioticus*. Mol. Microbiol. *28*, 1177–1185.
20. Volchegursky, Y., Hu, Z., Katz, L., and McDaniel, R. (2000). Biosynthesis of the anti-parasitic agent megalomicin: transformation of erythromycin to megalomicin in *Saccharopolyspora erythraea*. Mol. Microbiol. *37*, 752–762.
21. Xue, Y., Zhao, L., Liu, H.W., and Sherman, D.H. (1998). A gene cluster for macrolide antibiotic biosynthesis in *Streptomyces venezuelae*: architecture of metabolic diversity. Proc. Natl. Acad. Sci. USA *95*, 12111–12116.
22. Peschke, U., Schmidt, H., Zhang, H.Z., and Piepersberg, W. (1995). Molecular characterization of the linchmycin-production gene cluster of *Streptomyces linchlnensis* 78–11. Mol. Microbiol. *16*, 1137–1156.
23. Zhao, L., Borisova, S., Yeung, S.-M., and Liu, H.-W. (2001). Study of C-4 deoxygenation in the biosynthesis of desosamine: evidence implicating a novel mechanism. J. Am. Chem. Soc. *123*, 7909–7910.
24. Dutka-Malen, S., Mazodier, P., and Badet, B. (1988). Molecular cloning and overexpression of the glucosamine synthetase gene from *Escherichia coli*. Biochimie *70*, 287–290.
25. Zhao, L., Que, N.L.S., Xue, Y., Sherman, D.H., and Liu, H.-W. (1998). Mechanistic studies of desosamine biosynthesis: C-4 deoxygenation precedes C-3 transamination. J. Am. Chem. Soc. *120*, 12159–12160.
26. Thorson, J.S., Hosted, T.J., Jr., Jiang, J., Biggins, J.B., and Ahlert, J. (2001). Nature's carbohydrate chemistry: the enzymatic glycosylation of bioactive bacterial metabolites. Curr. Org. Chem. *5*, 139–167.
27. El Zoeiby, A., Sanschagrin, F., and Levesque, R.C. (2003). Structure and function of the Mur enzymes: development of novel inhibitors. Mol. Micorobiol. *47*, 1–12.
28. Danese, P.N., Oliver, G.R., Barr, K., Bowman, G.D., Rick, P.D., and Silhavy, T.J. (1998). Accumulation of the enterobacterial common antigen lipid II biosynthetic intermediate stimulates *degP* transcription in *Escherichia coli*. J. Bacteriol. *180*, 5875–5884.
29. Rahman, A., Barr, K., and Rick, P.D. (2001). Identification of the structural gene for the TDP-Fuc4NAc:lipid II Fuc4NAc transferase involved in synthesis of enterobacterial common antigen in *Escherichia coli* K-12. J. Bacteriol. *183*, 6509–6516.
30. Agrawal, P.K. (1992). NMR spectroscopy in the structural elucidation of oligosaccharides and glycosides. Phytochemistry *31*, 3307–3330.
31. Wang, L., and Reeves, P.R. (1998). Organization of *Escherichia coli* O157 O antigen gene cluster and identification of its specific genes. Infect. Immun. *66*, 3545–3551.
32. Mehta, P.K., Hale, T.I., and Christen, P. (1989). Evolutionary relationships among aminotransferases. Tyrosine aminotransferase, histidinol-phosphate aminotransferase, and aspartate aminotransferase are homologous proteins. Eur. J. Biochem. *186*, 249–253.
33. Mehta, P.K., Hale, T.I., and Christen, P. (1993). Aminotransferases: demonstration of homology and division into evolutionary subgroups. Eur. J. Biochem. *214*, 549–561.
34. Jensen, R.A., and Gu, W. (1996). Evolutionary recruitment of biochemically specialized subdivisions of family I within the protein superfamily of aminotransferases. J. Bacteriol. *178*, 2161–2171.
35. Akabayashi, A., and Kato, T. (1989). One-step and two-step fluorometric assay methods for general aminotransferases using glutamate dehydrogenase. Anal. Biochem. *182*, 129–135.
36. Godfroid, F., Taminiau, B., Danese, I., Denoel, P., Tibor, A., Weynants, V., Cloeckaert, A., Godfroid, J., and Letesson, J.J. (1998). Identification of the perosamine synthetase gene of *Brucella melitensis* 16M and involvement of lipopolysaccharide O side chain in *Brucella* survival in mice and in macrophages. Infect. Immun. *66*, 5485–5493.
37. Awram, P., and Smit, J. (2001). Identification of lipopolysaccharide O antigen synthesis genes required for attachment of the S-layer of *Caulobacter crescentus*. Microbiol. *147*, 1451–1460.
38. Powell, J.T., and Morrison, J.F. (1978). The purification and properties of the aspartate aminotransferase and aromatic-amino-acid aminotransferase from *Escherichia coli*. Eur. J. Biochem. *87*, 391–400.
39. Lain-Guelbenzu, B., Cardenas, J., and Munoz-Blanco, J. (1991). Purification and properties of L-alanine aminotransferase from *Chlamydomonas reinhardtii*. Eur. J. Biochem. *202*, 881–887.
40. Shin, J.-S., and Kim, B.-G. (1999). Asymmetric synthesis of chiral amines with -transaminase. Biotechnol. Bioeng. *65*, 206–211.
41. Yohana, K., Suzuki, K., Minei, H., and Toyama, S. (1983). Distribution of ω-amino acid:pyruvate transferase and aminobutyrate:α-ketoglutarate transaminase in microorganisms. Agric. Biol. Chem. *47*, 2257–2265.
42. Inoue, K., Kuramitsu, S., Aki, K., Watanabe, Y., Takagi, T., Nishigai, M., Ikai, A., and Kagamiyama, H. (1988). Branched-chain amino acid aminotransferase of *Escherichia coli*: overproduction and properties. J. Biochem. (Tokyo) *104*, 777–784.
43. Tanizawa, K., Masu, Y., Asano, S., Tanaka, H., and Soda, K. (1989). Thermostable D-amino acid aminotransferase from a thermophilic *Bacillus* species. Purification, characterization, and active site sequence determination. J. Biol. Chem. *264*, 2445–2449.
44. Okamoto, A., Nakai, Y., Hayashi, H., Hirotsu, K., and Kagamiyama, H. (1998). Crystal structures of *Paracoccus denitrificans* aromatic amino acid aminotransferase: a substrate recognition site constructed by rearrangement of hydrogen bond network. J. Mol. Biol. *280*, 443–461.
45. Shin, J.-S., and Kim, B.-G. (2002). Exploring the active site of amine:pyruvate aminotransferase on the basis of the substrate structure-reactivity relationship: how the enzyme controls sub-

strate specificity and stereoselectivity. J. Org. Chem. *67*, 2848–2853.
46. Hwang, B.-Y., Scheib, H., Pleiss, J., Kim, B.-G., and Schmid, R.D. (2000). Computer-aided molecular modeling of the enantioselectivity of *Pseudomonas cepacia* lipase toward γ- and δ-lactones. J. Mol. Catal., B Enzym. *10*, 223–231.
47. Noland, B.W., Newman, J.M., Hendle, J., Badger, J., Christopher, J.A., Tresser, J., Buchanan, M.D., Wright, T.A., Rutter, M.E., Sanderson, W.E., et al. (2002). Structural studies of *Salmonella typhimurium* ArnB (PmrH) aminotransferase: a 4-amino-4-deoxy-L-arabinose lipopolysaccharide-modifying enzyme. Structure *10*, 1569–1580.
48. Weinreich, M., Liang, C., and Stillman, B. (1999). The Cdc6p nucleotide-binding motif is required for loading mcm proteins onto chromatin. Proc. Natl. Acad. Sci. USA *96*, 441–446.
49. Shin, J.-S., and Kim, B.-G. (2001). Comparison of the omega-transaminases from different microorganisms and application to production of chiral amines. Biosci. Biotechnol. Biochem. *65*, 1782–1788.
50. Vernal, J., Cazzulo, J.J., and Nowicki, C. (1998). Isolation and partial characterization of a broad specificity aminotransferase from *Leishmania mexicana* promastigotes. Mol. Biochem. Parasitol. *96*, 83–92.
51. Gunn, J.S., Ryan, S.S., Van Velkinburgh, J.C., Ernst, R.K., and Miller, S.I. (2000). Genetic and functional analysis of a PmrA-PmrB-regulated locus necessary for lipopolysaccharide modification, antimicrobial peptide resistance, and oral virulence of *Salmonella enterica* serovar typhimurium. Infect. Immun. *68*, 6139–6146.
52. Tamegai, H., Nango, E., Kuwahara, M., Yamamoto, H., Ota, Y., Kuriki, H., Eguchi, T., and Kakinuma, K. (2002). Identification of L-glutamine: 2-deoxy-scyllo-inososе aminotransferase required for the biosynthesis of butirosin in *Bacillus circulans*. J. Antibiot. (Tokyo) *55*, 707–714.
53. Oh, J., Kim, B.-G., Lee, S.-G., Sohng, J.K., Liou, K., and Lee, H.C. (2003). One-pot enzymatic production of dTDP-4-keto-6-deoxy-D-glucose from dTMP. Biotechnol. Bioeng. *84*, 452–458.
54. Laemmli, U.K. (1970). Cleavage of structural proteins during the assembly of the head of bacteriophage T4. Nature *227*, 680–685.
55. Bradford, M.M. (1976). A rapid and sensitive method for the quantitation of microgram quantities of protein utilizing the principle of protein-dye binding. Anal. Biochem. *72*, 335–339.
56. Altschul, S.F., Gish, W., Miller, W., Myers, E.W., and Lipman, D.J. (1990). Basic local alignment search tool. J. Mol. Biol. *215*, 403–410.
57. Altschul, S.F., Madden, T.L., Schaffer, A.A., Zhang, J., Zhang, Z., Miller, W., and Lipman, D.J. (1997). Gapped BLAST and PSI-BLAST: a new generation of protein database search programs. Nucleic Acids Res. *25*, 3389–3402.
58. Thompson, J.D., Gibson, T.J., Plewniak, F., Jeanmougin, F., and Higgins, D.G. (1997). The CLUSTAL_X windows interface: flexible strategies for multiple sequence alignment aided by quality analysis tools. Nucleic Acids Res. *25*, 4876–4882.
59. Higgins, D.G., and Sharp, P.M. (1988). CLUSTAL: a package for performing multiple sequence alignment on a microcomputer. Gene *73*, 237–244.